Cement and Concrete Research 65 (2014) 8–14

Contents lists available at ScienceDirect

Cement and Concrete Research

journal homepage: http://ees.elsevier.com/CEMCON/default.asp

Formation of magnesium silicate hydrate (M-S-H) cement pastes using sodium hexametaphosphate

Tingting Zhang [a,b,c], Luc J. Vandeperre [b], Christopher R. Cheeseman [c,*]

[a] Faculty of Infrastructure Engineering, Dalian University of Technology, Dalian 116024, China
[b] Department of Materials, Centre for Advanced Structural Ceramics, Imperial College London, South Kensington Campus, London SW7 2AZ, UK
[c] Department of Civil and Environmental Engineering, Imperial College London, South Kensington Campus, London SW7 2AZ, UK

ARTICLE INFO

Article history:
Received 25 February 2014
Accepted 9 July 2014
Available online 1 August 2014

Keywords:
Dispersion (A)
Hydration products (B)
Compressive strength (C)
MgO (D)
Silica fume (D)

ABSTRACT

Magnesium silicate hydrate (M-S-H) gel is formed by the reaction of brucite with amorphous silica during sulphate attack in concrete and M-S-H is therefore regarded as having limited cementing properties. The aim of this work was to form M-S-H pastes, characterise the hydration reactions and assess the resulting properties. It is shown that M-S-H pastes can be prepared by reacting magnesium oxide (MgO) and silica fume (SF) at low water to solid ratio using sodium hexametaphosphate (NaHMP) as a dispersant. Characterisation of the hydration reactions by x-ray diffraction and thermogravimetric analysis shows that brucite and M-S-H gel are formed and that for samples containing 60 wt.% SF and 40 wt.% MgO all of the brucites react with SF to form M-S-H gel. These M-S-H cement pastes were found to have compressive strengths in excess of 70 MPa.

1. Introduction

It is well known that magnesium-silicate-hydrate (M-S-H) gels form as a result of sulphate attack of concrete in the presence of magnesium ions [1]. M-S-H is present during the later stages of sulphate attack and hence M-S-H gels are generally believed to be of limited strength [2,3]. As a result, M-S-H gel has received little attention as a potential cementing phase. Brew and Glasser [4,5] characterised chemically synthesised M-S-H gels and investigated the incorporation of caesium and potassium. Vandeperre et al. [6,7] recognised the possibility that brucite ($Mg(OH)_2$), which forms as the hydration product in reactive MgO cements, could react with the amorphous silica present in pulverised fuel ash (PFA) to form M-S-H, but were unable to confirm its presence. It is possible that identification of M-S-H gel by x-ray diffraction (XRD) was hampered by the large amorphous background and multiple crystalline phases present in PFA, which made it difficult to discern changes present in the amorphous phases. The pH of M-S-H based cement systems was studied in detail by Zhang et al. [8,9] during a work on the encapsulation of nuclear wastes containing trace metal contaminants.

The aim of this work was to establish if brucite and amorphous silica can react to give M-S-H gel, and to clearly determine whether this has potential as a cementing phase. It is known from a work on reactive MgO cements that the water demand of fine, light burned, MgO powders tends to be high, and that coarser MgO powders produced by calcining at higher temperatures which have lower water demand, cause damage due to expansion during late hydration [6]. The same problem of high water demand was encountered in early trials during this work, resulting in long setting times and low compressive strengths (<2 MPa) [10]. Therefore the first point that needed to be addressed was the rheology of the MgO/SF pastes. It has been reported that inorganic phosphate salts, sodium hexametaphosphate (NaHMP) and potassium hexametaphosphate (KHMP) improve the fluidity of MgO-micro-silica systems [11]. Therefore in this work the effect of NaHMP addition on the MgO/SF system has been investigated.

The structure of NaHMP, $(NaPO_3)_6$, is shown in Fig. 1. It is used in the manufacture of soap, metal finishing, water treatment, detergents and metal plating [12,13]. NaHMP is also widely used as a deflocculant for clays. The deflocculant effect occurs by increasing the negative charge on clay micelles. It is also adsorbed as an anion to give complexes with the flocculant cations and substitutes the cations in the double layer of the clay with Na^+ ions [14]. Studies have also shown that NaHMP can significantly reduce the adverse effect of serpentine on the flotation of pyrite to allow serpentine to disperse in alkaline conditions and this improves the adsorption of xanthate on pyrite [15]. Therefore, initial experiments determined the optimum addition level of NaHMP and in the remainder of the paper the effect of water to solid ratio on phase formation and strength development is reported.

* Corresponding author. Tel.: +44 207 594 5971.
E-mail address: c.cheeseman@imperial.ac.uk (C.R. Cheeseman).

http://dx.doi.org/10.1016/j.cemconres.2014.07.001

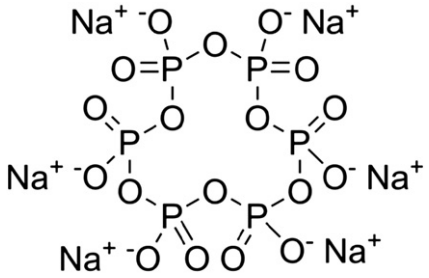

Fig. 1. Structure of sodium hexametaphosphate (NaHMP).

2. Experimental methods

The materials and chemicals used to prepare the cement mixtures were commercially available magnesium oxide (MgO, MagChem 30, M.A.F. Magnesite B.V., The Netherlands), silica fume (SF; Elkem Materials Ltd, UK) and sodium hexametaphosphate (NaHMP, Fisher, UK). The characteristics of the raw materials as reported by the suppliers are summarised in Table 1. The particle size distribution of the raw materials was analysed by laser diffraction in a water medium (Beckman Coulter LS-100) over the size range 0.4–900 μm. To improve dispersion of single particles, samples were sonicated before the measurement. Despite this precaution, the size is large relative to the specific surface area, suggesting the powder is agglomerated.

Previous work on characterisation of laboratory synthesised M-S-H gels has shown that such gels can form with a magnesium to silicon ratio in the range 0.67 to 1 [4,5]. Therefore, it was decided to investigate a blend of 60 wt.% silica fume and 40 wt.% MgO, i.e. with an atomic Mg/Si ratio of 1. An advantage of working near this limit is that the lack of complete reaction should result in the presence of brucite, a crystalline phase which is easily detected using XRD relative to unreacted silica fume.

To optimize the concentration of the NaHMP, trials were conducted in which the amount of additive was varied between 0.4 and 1.1 wt.% relative to the solids content. A series of experiments were therefore completed to determine the optimum addition of Na-HMP to 40% MgO/60% SF samples. Before preparing each sample, a certain amount of Na-HMP (0.025, 0.05, 0.075, 0.1, 0.15, 0.2, 0.25, 0.3 and 0.35 g) was dissolved in 10 g of water and 40% MgO and 60% SF by weight were mixed as powder. During mixing of each sample, 40% MgO/60% SF powder was added into the solution in steps of 0.5 g and thoroughly hand mixed. The addition of powder was continued until the mixture was no-longer a paste. The total amount of powder addition into each sample was recorded and the w/s ratio and Na-HMP content calculated.

For further work the dispersant addition was set at the lowest level that reduced the water content as much as possible. Hence, a range of pastes with water/solid ratios ranging from 0.4 to 0.8 was prepared using 1 wt.% NaHMP. Samples were cast in steel moulds to give 25 mm × 25 mm × 25 mm samples which were cured in sealed boxes with a relative humidity of >98% RH to avoid samples from drying during curing.

The evolution of the hydration was studied by XRD and by thermogravimetric analysis. XRD (PW 1700 with Cu Kα radiation, Philips, The Netherlands) was used to identify the crystalline phases present in samples. Experiments were performed in the 2θ range between 5° and 70°. Common x-ray diffraction data bases do not contain information on the x-ray diffraction response of M-S-H gels, which are poorly crystalline. Therefore, it was decided to produce a reference sample of M-S-H gel following the synthetic route developed by Brew and Glasser [4] in which solutions of water-glass ($Na_2SiO_3 \cdot 5H_2O$, Fisher, UK) and magnesium nitrate ($Mg(NO_3)_2 \cdot 6H_2O$, Fisher, UK) were cooled to 0 °C and mixed by stirring in a three-necked flask at a 1:1 Mg/Si ratio. The flask was kept immersed in an ice-water bath during the precipitation process. The $Mg(NO_3)_2 \cdot 6H_2O$ was slowly added to the $Na_2SiO_3 \cdot 5H_2O$ solution. The precipitate formed was filtered and washed five times to remove all the sodium ions and then dried in a desiccator at 20 °C for 7 days prior to XRD.

Combined TGA/DTA (Netzsch-STA) was used in this research with the sample weight fixed at ~20 mg for all solid samples with a sample particle size of <1 mm. The tests were performed under a nitrogen flow of 58 ml/min with a heating rate of 10 °C/min. The weight loss was measured by the tangent method. To enable quantification of the phases present, the pure M-S-H gel produced as a reference for XRD was also analysed after drying to 200 °C. The compressive strength was determined after 7, 14, 28 and 90 days on wet cube samples with edge length of 25 mm.

Table 1
Characterisation data for MgO and silica fume.

	MgO wt.%	Silica fume wt.%
SiO_2	0.35	>97.5
Al_2O_3	0.1	<0.7
Fe_2O_3	0.15	<0.3
CaO	0.8	<0.3
P_2O_5	(n/a)	<0.1
MgO	98.2	<0.5
K_2O	(n/a)	<0.6
Na_2O	(n/a)	<0.3
SO_3	0.05	<0.4
Specific gravity ($g \cdot cm^{-3}$)	3.23	1.94
Mean particle size (μm)	5	21.3
BET surface area ($m^2 \cdot g^{-1}$)	25	21.4

3. Results and discussion

Fig. 2 shows that with increasing addition of NaHMP, the amount of water needed to allow a paste to be obtained reduces markedly up to 1 wt.% of NaHMP. Higher additions did not result in further reductions in water. Therefore, the optimum NaHMP addition used was 1 wt.%. This allowed pastes to be produced with water to solid ratio as low as 0.4.

Fig. 3 illustrates the strength development of samples with different water to solid ratios. It is clear that the compressive strength of 40% MgO/60% SF samples increases with time for all w/s ratios, which indicates hydration is ongoing throughout 90 days. It is also apparent that the compressive strength of 40% MgO/60% SF samples is significantly increased as the w/s ratio is reduced. The 28 day compressive strength of 40% MgO/60% SF samples with w/s 0.4 and w/s 0.5 is over 60 MPa, which is comparable to PC (CEM II, 42.5R) paste which has a typical compressive strength of 56 MPa at w/s 0.35. The rate of strength development is similar to that of alite (C_3S), as a large fraction of the strength is rapidly produced [16]. The water to solid ratio has a dramatic

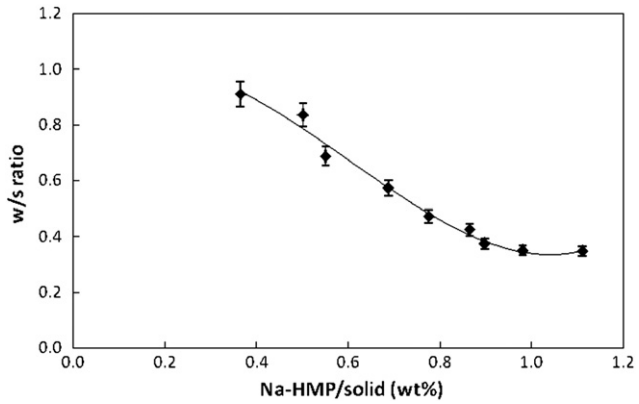

Fig. 2. Lowest w/s ratio at which a paste formed for different NaHMP additions.

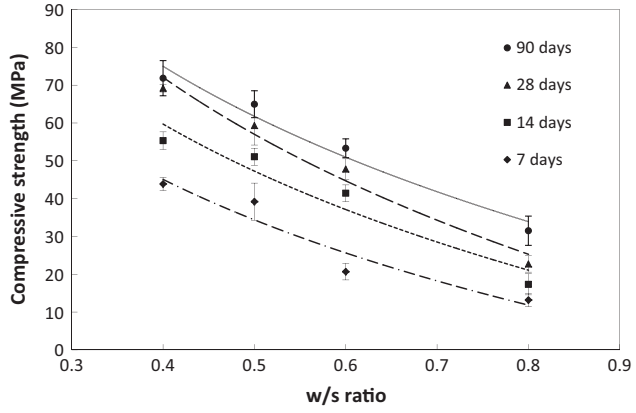

Fig. 3. Compressive strength of 40% MgO/60% SF samples with 1% NaHMP at different w/s ratios after 7, 14, 28 and 90 days.

influence on the strength and this is because excess water in cement paste increases porosity which weakens the material [7,16–19]. The high strength (>70 MPa) obtained at low water to solid ratio (0.4) indicates that M-S-H gel is a potential phase for developing strong products.

XRD patterns of the raw materials MgO and SF are shown in Fig. 4(a) and (b), and the XRD patterns of M-S-H gel prepared by the chemical method are presented in Fig. 4(c). The broad amorphous peaks for the product were found to be consistent with the XRD pattern of magnesium-silicate-hydrate (M-S-H) gel published by Brew and Glasser [4]. XRD pattern of 40% MgO/60% SF samples with different w/s ratios (Fig. 5) shows that two broad peaks at 2θ ~35° and ~60° appear after 28 days for different w/s ratios. This agrees well with the XRD data for the synthetically prepared M-S-H gel in Fig. 4(c) [4,5]. Hence these are due to the formation of M-S-H gel. Note that these poorly crystalline features become more clearly defined with time. This indicates that for all w/s ratios studied, the main hydration product of the 40% MgO/60% SF system is M-S-H gel.

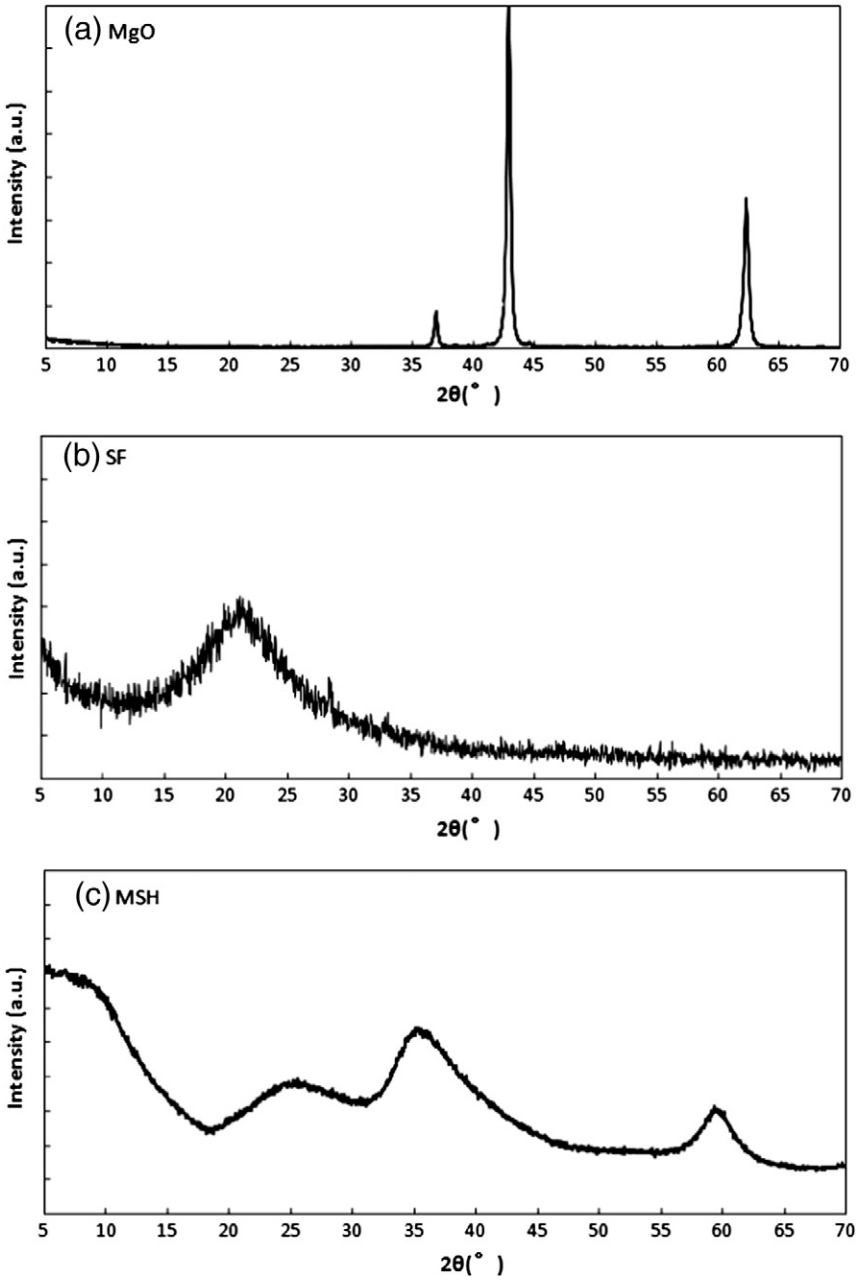

Fig. 4. X-ray diffraction data for pure materials (a) MgO, (b) SF and (c) MSH.

As presented in Fig. 5, for 40% MgO/60% SF binder at w/s ratios 0.4 and 0.5, both MgO and brucite ($Mg(OH)_2$) peaks decrease with time. However, even after 285 days, a significant amount of unreacted MgO remains. Data for samples with w/s ratios of 0.6 and 0.8 show that only poorly crystalline hydration products remain after 90 days and 285 days respectively. In contrast for the lowest w/s ratio the MgO peaks are very clear at 28 days and the brucite peaks are weaker than for samples with higher w/s ratio. Hence hydration is facilitated by the presence of more water. The brucite peaks decrease with time and disappear after 285 days which indicates that brucite continues to react with SF to form M-S-H gel. MgO also decreases with time, although some still remains after 285 days as shown in Fig. 5(c). MgO was the main crystalline phase in 40% MgO/60% SF samples with w/s 0.4 and w/s 0.5. This shows that brucite has reacted with SF to form M-S-H gel and because there is not enough water in the system or because hydration products form a barrier on the MgO particles, the remaining MgO cannot react to form brucite or react with SF to form M-S-H gel.

To further investigate and quantify the hydration products, TGA and DTA were used to measure the weight change of 40% MgO/60% SF samples (1% NaHMP) with different w/s ratios as the temperature is increased. Samples were heated to 1000 °C at a heating rate of 10 °C/min. Only samples with w/s = 0.5 and w/s = 0.8 were selected for TGA because these represent high and low water content mixes. The M-S-H gel prepared by the chemical method used by Brew and Glasser was also analysed. The TG-DTA data for M-S-H gel is presented in Fig. 8.

The TGA and DTA results of 40% MgO/60% SF with w/s = 0.5 and w/s = 0.8 after different curing times are shown in Figs. 6 and 7 respectively. Irrespective of the water content an endothermic peak occurs

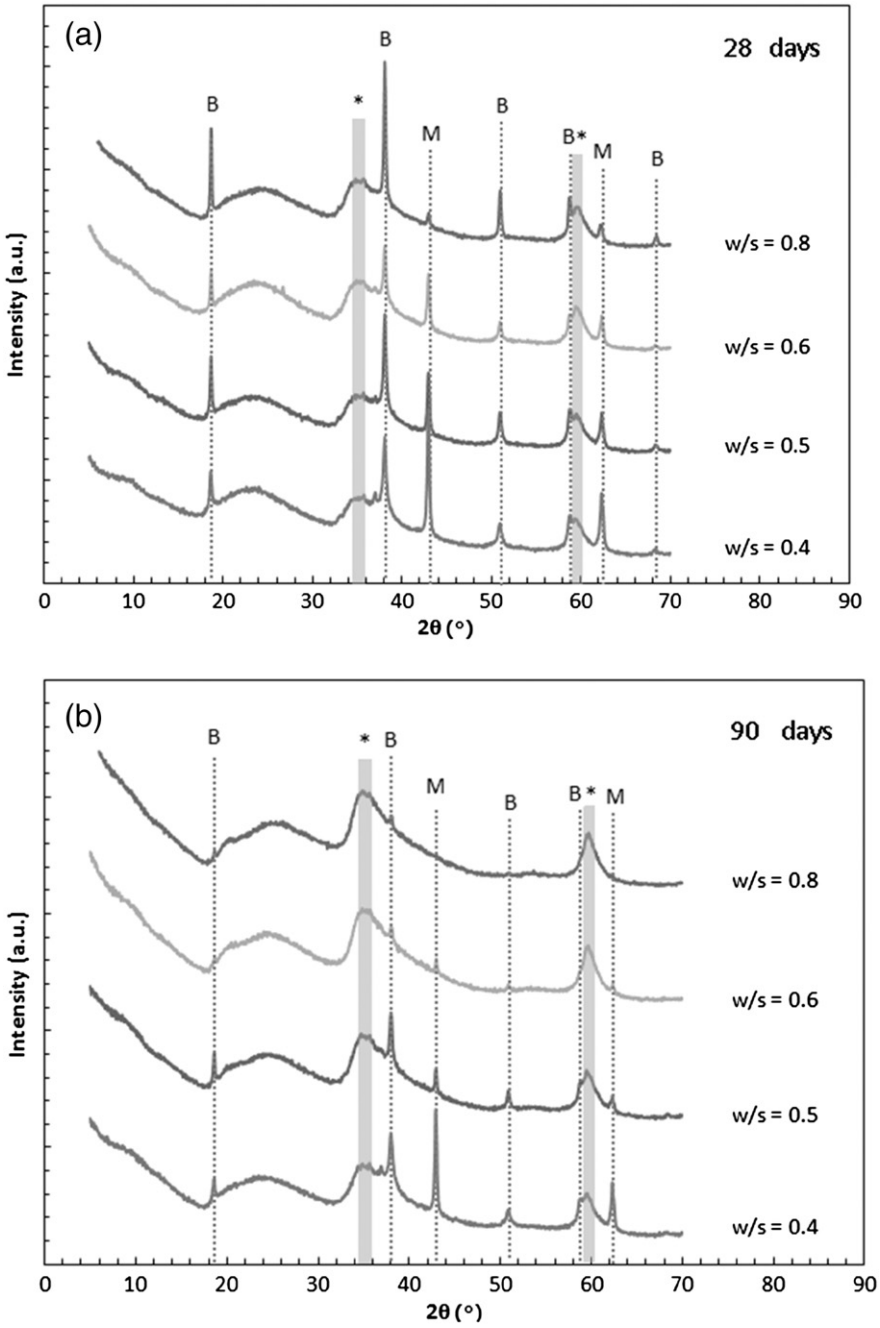

Fig. 5. X-ray diffraction data for blends of 60 wt.% silica fume and 40 wt.% MgO with different water to solid ratios after (a) 28 days, (b) 90 days and (c) 285 days curing. 1 wt.% of NaHMP was added to all blends. Crystalline peaks for magnesium hydroxide (brucite, B) and magnesium oxide (Periclase, M)are indicated. Most of the broad peaks are due to MSH gel (*), but silica fume also contributes to the broad peak between 18 and 30° 2θ.

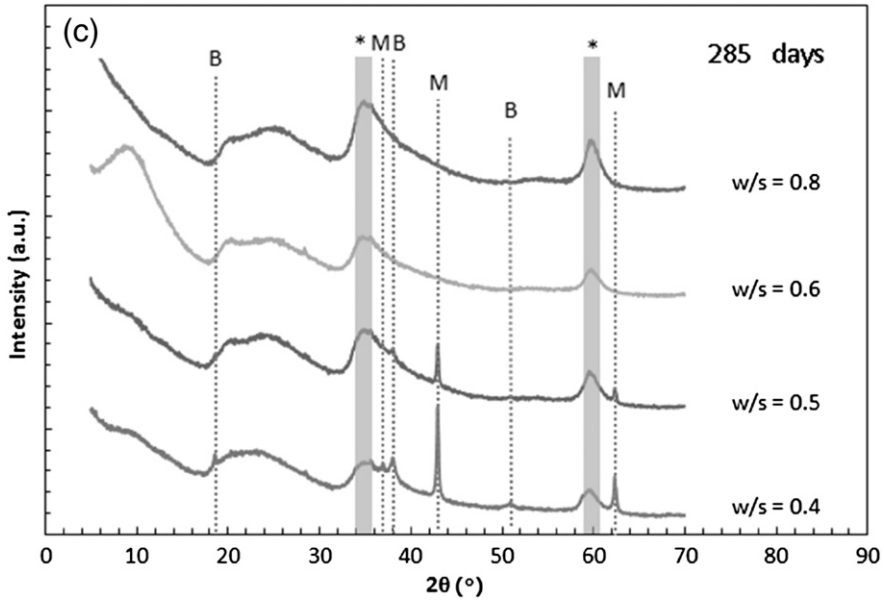

Fig. 5 (*continued*).

between 100 °C and 200 °C in 40% MgO/60% SF samples at all ages. This is believed to be caused by the weight loss of pore water and water contained in M-S-H gel. An exothermic peak at around 850 °C was observed in all 40% MgO/60% SF samples and its strength increases with curing time. This peak is therefore ascribed to crystallisation of the M-S-H gel into $MgSiO_3$, as explained below. The increase in strength of this peak indicates that hydration and M-S-H formation was ongoing during the test period. Both the exothermic and endothermic peaks were sharper in the 40% MgO/60% SF samples with higher water content (w/s = 0.8). This is consistent with the XRD results as more M-S-H gel was formed in samples with higher w/s ratio. Due to experimental

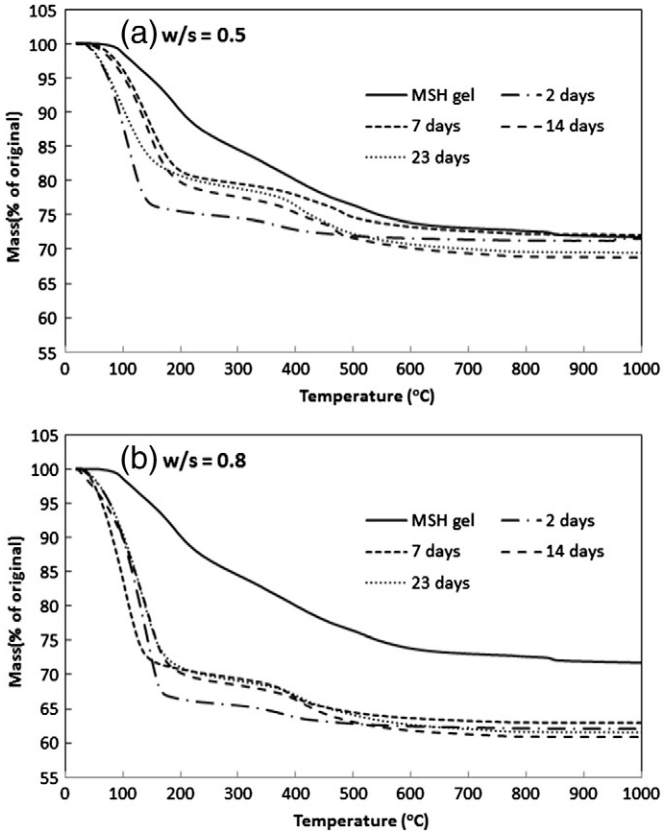

Fig. 6. TGA data of 40% MgO/60% SF (1% NaHMP) with (a) w/s = 0.5 and (b) w/s = 0.8 after 2, 7, 14 and 23 days curing and compared with M-S-H gel.

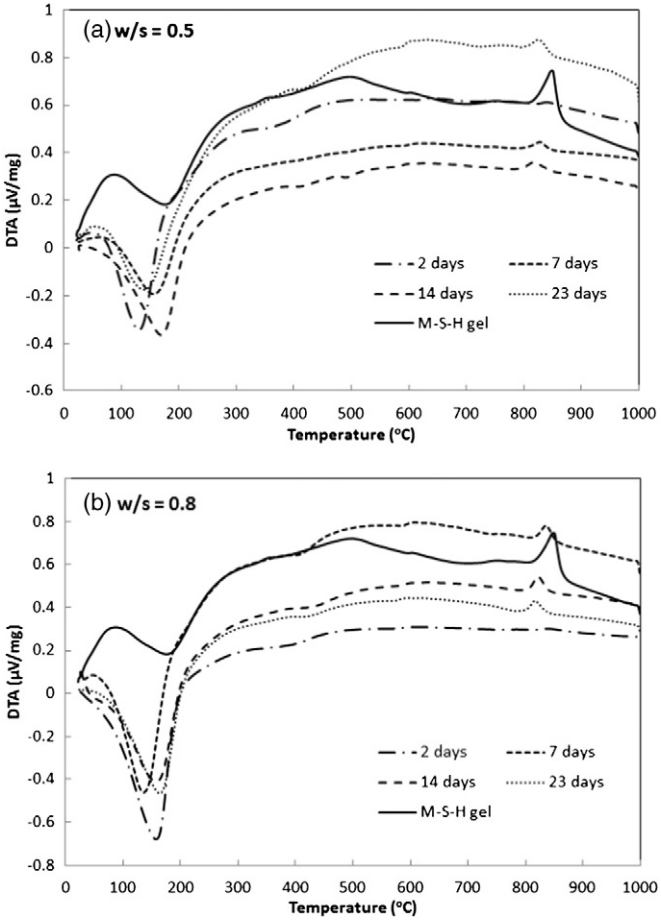

Fig. 7. DTA data of 40% MgO/60% SF (1% NaHMP) with (a) w/s = 0.5 and (b) w/s = 0.8 after 2, 7, 14 and 23 days curing and compared with M-S-H gel.

Table 2
Weight loss of 40% MgO/60% SF (1% NaHMP) with w/s = 0.5 and w/s 0.8 compared with M-S-H gel when heated to 1000 °C at 10 °C/min.

Description	Curing time	Weight loss (% of original)			
		20–200 °C	200–500 °C	500–1000 °C	Total
M-S-H gel	–	9.16	12.85	4.39	26.40
40% MgO/60% SF (w/s = 0.5)	2 days	23.72	2.97	0.49	27.18
	7 days	18.10	6.42	2.37	26.89
	14 days	19.47	8.06	2.95	30.48
	23 days	18.02	7.78	2.66	28.47
40% MgO/60% SF (w/s = 0.8)	2 days	32.96	3.25	0.61	36.82
	7 days	27.70	5.60	1.29	34.59
	14 days	28.89	6.75	2.20	37.84
	23 days	28.13	6.77	2.60	37.50

variations in sample sizes and time delays before each test, which lead to weight losses due to room temperature drying, the total weight loss did not vary in a systematic way with hydration time.

The weight loss of samples at each stage and the total weight loss are summarised in Table 2. Three stages of weight loss are identified:

a) 20 to 200 °C, weight loss of pore water and water locked up in M-S-H gel;
b) 200 to 500 °C, weight loss of water bonded to M-S-H gel and decomposition of brucite;
c) 500 to 1000 °C, weight loss of hydroxyl groups in M-S-H gel.

Table 2 shows that for both 40% MgO/60% SF samples with w/s 0.5 and w/s 0.8, the 500–1000 °C weight loss is increasing with curing time. This matches with the exothermic peaks shown in the DTA curves around 850 °C, which indicates that M-S-H gel is forming over the test period. However, there is only 0.49–0.61% weight loss between 500 and 1000 °C in both samples after 2 days, which indicates the main formation of M-S-H gel is principally at later curing times (>2 days). The weight losses of both samples are stable after 7 days in 20–200 °C and 200–500 °C.

The TG-DTA curve of 40% MgO/60% SF with w/s = 0.8 after 285 days curing and 24 h of drying at 105 °C is compared with that of M-S-H gel in Fig. 8. The total weight loss between 20 °C and 1000 °C is similar, but M-S-H gel has less weight loss between 20 and 200 °C. The weight loss between 500 and 1000 °C is approximately the same as the weight loss of pure M-S-H gel. XRD also shows that only M-S-H gel is present in this sample.

Based on the three stage weight loss assumptions and the 285 days TGA data, a formula of M-S-H gel formed can be calculated as $Mg_8Si_8O_{20}(OH)_8 \cdot 12H_2O$. The reaction is shown in Eq. (1).

$$8MgO + 8SiO_2 + 16H_2O \rightarrow M_8Si_8O_{20}(OH)_8 \cdot 12H_2O. \quad (1)$$

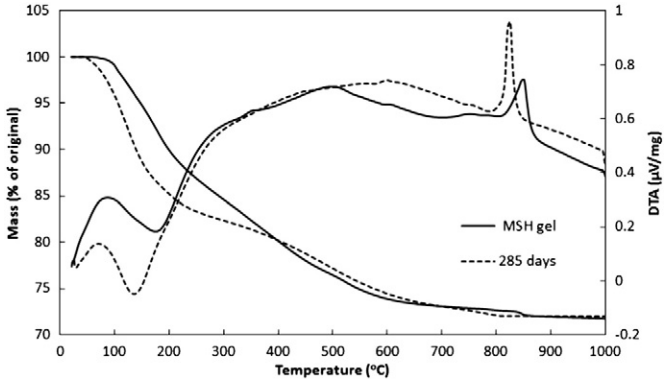

Fig. 8. TGA and DTA data of 40% MgO/60% SF (1% NaHMP) with w/s = 0.8 after 285 days curing and 24 h drying at 105 °C, compared with M-S-H gel.

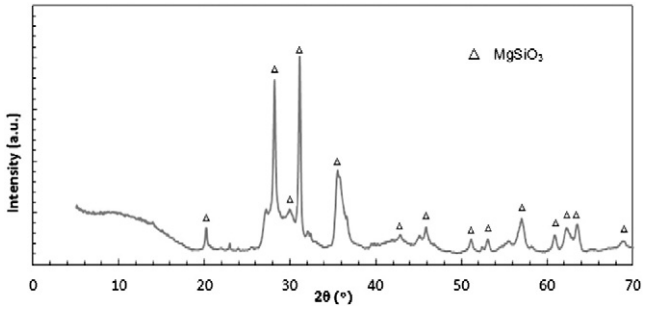

Fig. 9. XRD of 40% MgO/60% SF (1%NaHMP) with w/s = 0.5 after 28 days curing and 2 h of heating at 1100 °C (Δ:$MgSiO_3$).

According to this equation, a minimum w/s ratio of 0.36 is required to react with the 40% MgO/60% SF sample to form M-S-H gel. The weight loss observed indicates that 9 of the 12 waters are lost more readily than the remaining 3. A similar difference in water bonding is known to occur in crystalline hydrated sepiolite [20]. The XRD data in Fig. 9 confirms that $MgSiO_3$ was the only product left when 40% MgO/60% SF (1% NaHMP) with w/s = 0.5 was heated for 2 h at 1100 °C, which suggests the weight loss was caused by loss of water.

4. Conclusions

Addition of 1 wt.% of NaHMP reduces the water required for MgO/SF systems, which in turn improves the compressive strength dramatically (>70 MPa). This allows pastes to be produced with water to solid ratio as low as 0.4, which is similar to the standard w/s ratio for PC. Characterisation of the hydration by XRD and thermogravimetric analysis shows that hydration results in brucite and M-S-H gel formation, and that for mixtures containing 60 wt.% SF and 40 wt.% MgO over time all the brucites react with silica fume and converts into M-S-H gel, provided that sufficient water is present. Based on the 285 days TGA data of 40% MgO/60% SF sample with w/s 0.8, the formula of M-S-H gel formed can be calculated as $Mg_8Si_8O_{20}(OH)_8 \cdot 12H_2O$. This indicates the M-S-H gel formed in this research is probably a mixture of poorly crystallised sepiolite and serpentine.

Acknowledgement

This work was funded by the UK Engineering and Physical Sciences Research Council (EPSRC) through grant number EP/F055412/1, "DIAMOND: Decommissioning, Immobilization and Management of Nuclear wastes for Disposal" and "the Fundamental Research Funds for the Central Universities 'DUT12RC(3)74'" and KLSLRC (KLSLRC-KF-13-HX-9) in China.

References

[1] W.F. Cole, A crystalline hydrated magnesium silicate formed in the breakdown of a concrete sea-wall, Nature 171 (1953) 354–355.
[2] D. Bonen, Composition and appearance of magnesium silicate hydrate and its relation to deterioration of cement-based materials, J. Am. Ceram. Soc. 75 (1992) 2904–2906.
[3] J.W. Harrison, Tec-Cement Update, [cited 2010 31st March 2010]; Available from: http://www.tececo.com/files/conference_papers/Tec-CementUpdate301005.pdf 2005.
[4] D.R.M. Brew, F.P. Glasser, Synthesis and characterisation of magnesium silicate hydrate gels, Cem. Concr. Res. 35 (2005) 85–98.
[5] D.R.M. Brew, F.P. Glasser, The magnesia–silica gel phase in slag cements: alkali (K, Cs) sorption potential of synthetic gels, Cem. Concr. Res. 35 (2005) 77–83.
[6] L.J. Vandeperre, M. Liska, A. Al-Tabbaa, Reactive MgO cements: properties and applications, International Conference on Sustainable Construction Materials and Technologies, Taylor and Francis, Coventry, 2007.
[7] L.J. Vandeperre, M. Liska, A. Al-Tabbaa, Microstructures of reactive magnesia cement blends, Cement Concr. Compos. 30 (2008) 706–716.
[8] T. Zhang, L.J. Vandeperre, C.R. Cheeseman, Bottom-up design of a cement for nuclear waste encapsulation, Proceedings of the American Ceramic Society

35th International Conference on Advanced Ceramics and Composites, Daytona Beach, Florida, January 23–28 2011, pp. 41–48.
[9] T. Zhang, C.R. Cheeseman, L.J. Vandeperre, Development of low pH cement systems forming magnesium silicate hydrate (M-S-H), Cem. Concr. Res. 41 (2011) 439–442.
[10] T. Zhang, C.R. Cheeseman, L.J. Vandeperre, Development of novel low pH cement systems for encapsulation of wastes containing aluminium, Decommissioning, Immobilisation and Management of Nuclear Waste for Disposal, Diamond '09 Conference, 2009, (York).
[11] J. Wei, Q. Yu, W. Zhang, H. Zhang, Reaction products of MgO and microsilica cementitious materials at different temperatures, J. Wuhan Univ. Technol. 26 (2011) 745–748.
[12] S.T. Dybing, J.G. Parsons, J.H. Martin, K.R. Spurgeon, Effect of sodium hexametaphosphate on cottage cheese yields, J. Dairy Sci. 65 (1982) 544–551.
[13] H.K. Moudgil, S. Yadav, R.S. Chaudhary, D. Kumar, Synergistic effect of some antiscalants as corrosion inhibitor for industrial cooling water system, J. Appl. Electrochem. 39 (2009) 1339–1347.
[14] T. Manfredini, G.C. Pellacani, P. Pozzi, A.B. Corradi, Monomeric and oligomeric phosphates as deflocculants of concentrated aqueous clay suspensions, Appl. Clay Sci. 5 (1990) 193–201.
[15] Y. Lu, M. Zhang, Q. Feng, T. Long, L. Ou, G. Zhang, Effect of sodium hexametaphosphate on separation of serpentine from pyrite, Trans. Nonferrous Metals Soc. 21 (2010) 208–213.
[16] S. Mindess, J.F. Young, D. Darwin, Concrete, second ed. Prentice Hall, Upper Saddle River, 2003. 644.
[17] L.J. Vandeperre, M. Liska, A. Al-Tabbaa, Hydration and mechanical properties of magnesia, pulverized fuel ash, and Portland cement blends, J. Mater. Civ. Eng. 20 (2008) 375–383.
[18] P.C. Hewlett, Lea's Chemistry of Cement and Concrete, fourth ed., Arnold, London, 1998, p. 1053.
[19] A.M. Neville, Properties of Concrete, 2nd edition Pitman Publishing, London, 1973. 687.
[20] R.L. Frost, J. Kristof, E. Horvath, Controlled rate — thermal analysis of sepiolite, J. Therm. Anal. Calorim. 98 (2009) 749–755.